Current Biology 18, 926–931, June 24, 2008 ©2008 Elsevier Ltd All rights reserved DOI 10.1016/j.cub.2008.05.044

Report

MT1-MMP-Dependent Invasion Is Regulated by TI-VAMP/VAMP7

Anika Steffen,[1,2] Gaëlle Le Dez,[1,2] Renaud Poincloux,[1,2] Chiara Recchi,[1,2,7] Pierre Nassoy,[1,3] Klemens Rottner,[4] Thierry Galli,[5,6] and Philippe Chavrier[1,2,*]

[1]Institut Curie
Centre de Recherche
26 rue d'Ulm
75248 Paris
Cedex 05
France

[2]Membrane and Cytoskeleton Dynamics Group
UMR 144

[3]Physical Chemistry
UMR 168
Centre National de la Recherche Scientifique
75248 Paris
Cedex 05
France

[4]Cytoskeleton Dynamics Group
Helmholtz Centre for Infection Research
Inhoffen Straße 7
D-38124 Braunschweig
Germany

[5]Membrane Traffic in Neuronal and Epithelial Morphogenesis
INSERM Avenir Team
75005 Paris
France

[6]Institut Jacques Monod
Centre National de la Recherche Scientifique
UMR 7592
Universities Paris 6 and 7
75005 Paris
France

Summary

Proteolytic degradation of the extracellular matrix (ECM) is one intrinsic property of metastatic tumor cells to breach tissue barriers and to disseminate into different tissues. This process is initiated by the formation of invadopodia, which are actin-driven, finger-like membrane protrusions. Yet, little is known on how invadopodia are endowed with the functional machinery of proteolytic enzymes [1, 2]. The key protease MT1-MMP (membrane type 1-matrix metalloproteinase) confers proteolytic activity to invadopodia and thus invasion capacity of cancer cells [3–6]. Here, we report that MT1-MMP-dependent matrix degradation at invadopodia is regulated by the v-SNARE TI-VAMP/VAMP7, hence providing the molecular inventory mediating focal degradative activity of cancer cells. As observed by TIRF microscopy, MT1-MMP-mCherry and GFP-VAMP7 were simultaneously detected at proteolytic sites. Functional ablation of VAMP7 decreased the ability of breast cancer cells to degrade and invade in a MT1-MMP-dependent fashion. Moreover, the number of invadopodia was dramatically decreased in VAMP7- and MT1-MMP-depleted cells, indicative of a positive-feedback loop in which the protease as a cargo of VAMP7-targeted transport vesicles regulates maturation of invadopodia. Collectively, these data point to a specific role of VAMP7 in delivering MT1-MMP to sites of degradation, maintaining the functional machinery required for invasion.

*Correspondence: philippe.chavrier@curie.fr
[7]Present address: Molecular and Cellular Medicine, National Heart and Lung Institute, Imperial College London, London SW7 2AZ, United Kingdom

Results and Discussion

MT1-MMP Colocalizes with the v-SNARE VAMP7 at Focal Sites of Degradation

Among the matrix-proteinases, MT1-MMP has been widely shown to be required for matrix degradation and remodeling by invasive tumor cells [4, 6–9]. However, the dynamic and coordinated targeting of the transmembrane enzyme MT1-MMP by cytoplasmic factors to sites of degradation has been subject of little investigation. It is well established that MT1-MMP is rapidly endocytosed from the plasma membrane and reaches early and late endocytic structures ([10], [11], and our unpublished data). Endocytosis and recycling have been proposed as a mechanism for controlling MT1-MMP activity during matrix degradation [10–14], and recently, a Rab8-dependent pathway was also suggested to contribute to MT1-MMP exocytosis during collagen degradation [15].

We first set out to explore the subcellular localization of MT1-MMP, visualized as fluorescently tagged fusion protein (MT1-MMP-mCherry). MDA-MB-231 human breast cancer cells stably expressing MT1-MMP-mCherry (MDA-MT1ch cells, Sakurai-Yageta et al. [16]) were counterstained for EEA1 (early endosomal antigen 1) and LAMP1 (lysosomal-associated membrane protein 1), respectively (see Figure S1 available online). The majority of MT1-MMP-mCherry colocalized with the late endosome (LE)/lysosomal compartment marker LAMP1 (Figure S1B), whereas only few MT1-MMP-mCherry was found in early endosome (EE) compartments, as visualized by anti-EEA1 staining (Figure S1A).

It is so far unknown to what extent MT1-MMP trafficking from EE to LE/lysosomes might represent a degradative pathway for the protease [10]. Here, we rather wondered whether this accumulation of MT1-MMP in LE/lysosomal endocompartments could also reflect a storage pool that is involved in active translocation to the plasma membrane. This would require a specific fusion machinery regulating exocytosis of these endocompartments. SNARE (soluble NSF [N-ethylmaleimide-sensitive factor] attachment protein receptor) proteins constitute the basic machinery for membrane fusion, thereby acting in all membrane trafficking steps [17–19]. TI-VAMP/VAMP7 (referred to as VAMP7 herein) was identified as a vesicular (v-) SNARE mainly present on the TGN (trans-golgi network) and LE/lysosomal structures [20, 21] and was shown to contribute to neurite outgrowth [22, 23], GLUT4 release [24], apical targeting in polarized epithelial cells [20, 25], phagocytosis [26], and cytokinesis [27]. Altogether, these results led to the conclusion that VAMP7 is the v-SNARE responsible for LE/lysosomal exocytosis (for review, see [28]). VAMP7 staining in MDA-MT1ch cells (Figure 1A) revealed a high

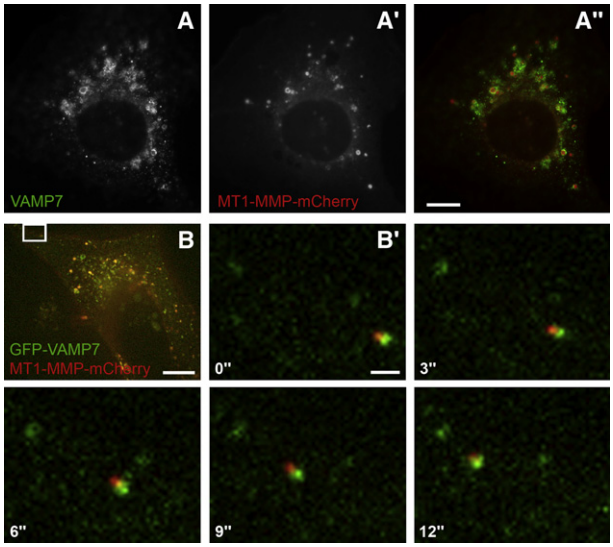

Figure 1. MT1-MMP Is Trafficking in VAMP7-Positive Compartments

(A–A″) MDA-MB-231 cells stably expressing MT1-MMP-mCherry ([A′] and [A″] in red) were counterstained for VAMP7 ([A] and [A″] in green).

(B) GFP-VAMP7 and MT1-MMP-mCherry are cotrafficking in MDA-MB-231 cells.

(B′) Time lapse of the boxed region in (B). Note that the slight shift of the mCherry/GFP signals is due to consecutive imaging of GFP-VAMP7 and MT1-MMP-mCherry (see also Movie S1). Time is given in seconds. The scale bar in (A″) and in (B) represent 10 μm. The scale bar in (B′) represents 1 μm.

degree of colocalization with MT1-MMP, corroborating localization of MT1-MMP to LE/lysosomal structures and raising the possibility that VAMP7 could regulate the fusion of MT1-MMP-containing endosomes with the plasma membrane. When analyzed by live-cell imaging, GFP-VAMP7 and MT1-MMP-mCherry expressed in MDA-MB-231 cells also displayed a high degree of colocalization in large static vesicular structures in the juxtanuclear region of the cells as well as in smaller, highly dynamic vesicles (Figures 1B and 1B′ and Movie S1).

When MDA-MT1ch cells were plated on fluorescently labeled crosslinked gelatin in an assay monitoring matrix degradation [4], regular epifluorescence imaging revealed in rare cases a weak signal of the protease (MT1-MMP-mCherry, see Figure 2F) at sites of degradation appearing as black holes in the fluorescent gelatin (Figure 2C). However, we were unable to detect GFP-VAMP7 at these sites (Figure 2E). In contrast, selective illumination of the ventral plasma membrane by TIRF microscopy showed a strong correlation between MT1-MMP-mCherry and sites of degradation (compare Figure 2B with Figure 2C). Furthermore, we found GFP-VAMP7 colocalizing and accumulating with the protease at the ventral plasma membrane at focal sites of proteolysis (Figures 2A–2D, 2G, and 2H). This suggests that although the proteolytic activity resulting in loss of fluorescence of gelatin is mediated by the protease MT1-MMP, the v-SNARE VAMP7 targets its cargo to focal sites of degradation. It should be noted that GFP-VAMP7 was neither always detected at (see also Figure 3D) nor restricted to degradative sites (Figure 2D, arrowhead). Because delivery of cargo is a dynamic process involving recycling of the fusion machinery, disappearance of the v-SNARE upon fusion by rapid recycling is likely. Moreover, we cannot exclude that VAMP7 may also transport other cargo(es) different from MT1-MMP. Nevertheless, the strong colocalization of GFP-VAMP7 with MT1-MMP-mCherry at sites of degradation

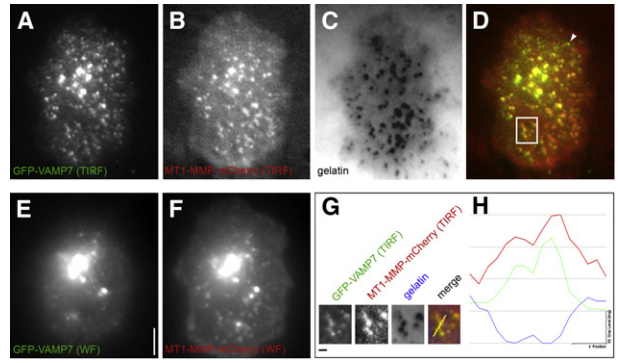

Figure 2. VAMP7 Colocalizes with MT1-MMP-mCherry at Focal Sites of Degradation

MDA-MB-231 cells ectopically expressing GFP-VAMP7 (A and E) and MT1-MMP-mCherry (B and F) on fluorescently labeled gelatin (C) were imaged by TIRF (A and B) and wide-field (WF) microscopy (E and F). In (D), a merged image of GFP-VAMP7 in green and MT1-MMP-mCherry in red by TIRF reveals a high degree of colocalization of both proteins at the ventral plasma membrane. The arrowhead points to a GFP-VAMP7 vesicle not colocalizing with MT1-MMP-mCherry and gelatin degradation. (G) shows enlargements of the boxed region in (D). In (H), measurements of fluorescent intensities on the line depicted in (G) on the merged image shows concomitant increase of intensities of GFP-VAMP7 (green line) and MT1-MMP-mCherry (red line) correlating with loss of fluorescent intensity of the gelatin (blue line). The scale bar in (E) (valid for [A]–[F]) represents 5 μm, and the scale bar in (G) represents 1 μm.

suggests that VAMP7 may be a critical v-SNARE delivering MT1-MMP to its site of action.

Time-lapse TIRF microscopy of MDA-MB-231 cells expressing MT1-MMP-mCherry and GFP-VAMP7 revealed a dynamic recruitment of GFP-VAMP7 to sites of degradation (Figures 3B–3E). Active sites of degradation were visible by loss of fluorescence of the gelatin (Figure 3C), and these sites corresponded with accumulations of vesicles of GFP-VAMP7 visualized by TIRF (Figures 3B and 3D), indicating that these vesicles are close to the ventral plasma membrane. Importantly, recruitment of GFP-VAMP7 vesicles to this site was observed (Figure 3E, arrow, and Movie S2). Upon dynamic recruitment to this site, these vesicles seemed to dock at this

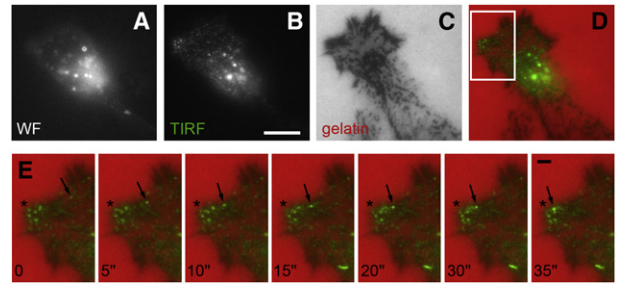

Figure 3. GFP-VAMP7 Is Dynamically Recruited to Active Sites of Proteolysis

GFP-VAMP7 was visualized by wide-field (WF) (A) and TIRF (B) microscopy in MDA-MB-231 cells coexpressing MT1-MMP-mCherry on fluorescently labeled gelatin (C). TIRF microscopy of GFP-VAMP7 (B) reveals small vesicles close to the ventral plasma membrane, whereas wide-field (A) microscopy visualizes bigger compartments in the cytoplasm. (D) shows a merged image of GFP-VAMP7 by TIRF (green) and gelatin (red). (E) shows a time lapse of the boxed region in (D). The arrow indicates movement of a GFP-VAMP7 vesicle toward an accumulation of vesicles marked by an asterisk at sites of degradation (see also Movie S2). Time is given in seconds. The scale bar in (B) (valid for [A]–[D]) represents 10 μm; the scale bar in (E) represents 2 μm.

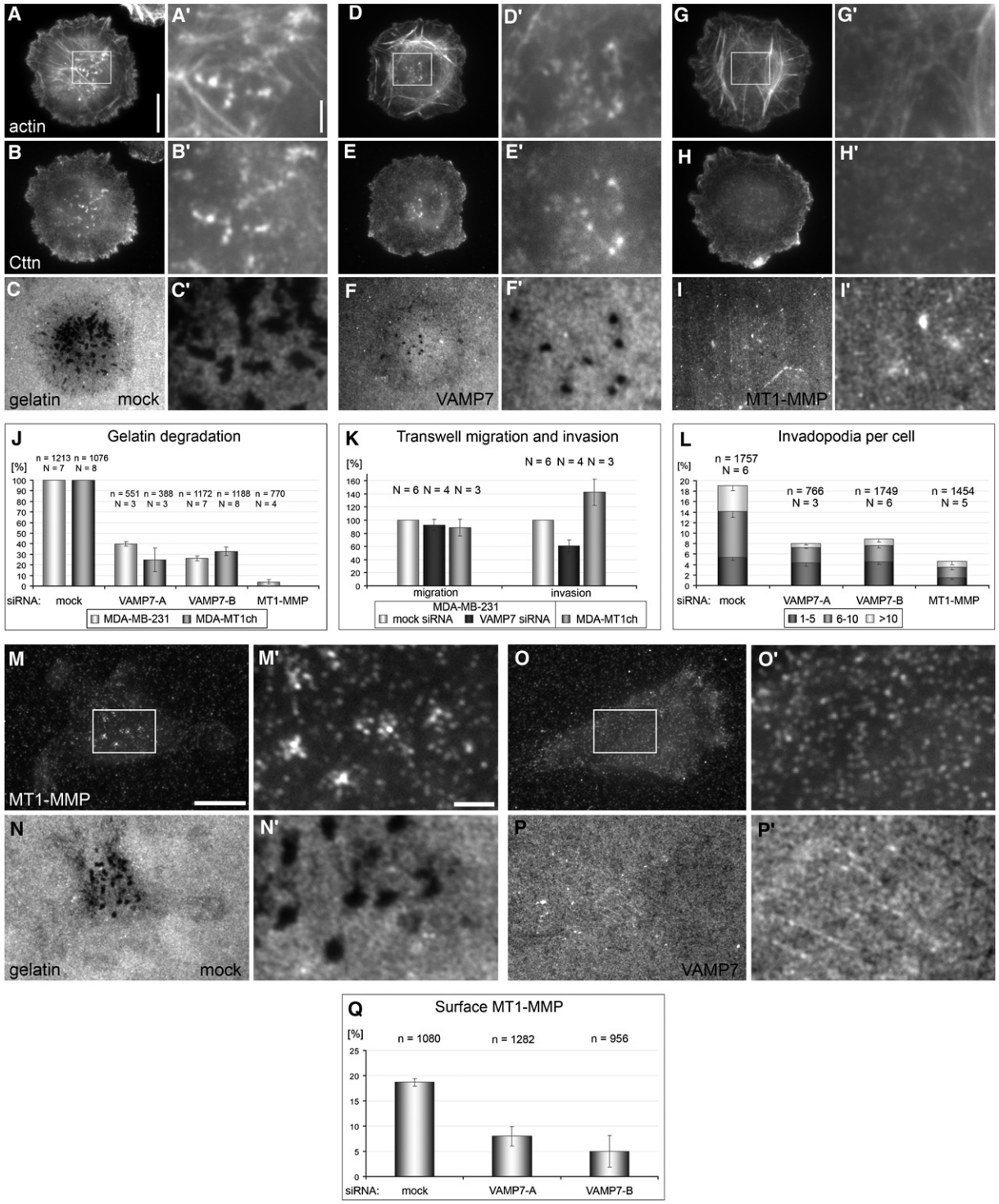

Figure 4. Interference with VAMP7 Expression Impairs Degradation Capacities of Breast Cancer Cells through Reduced MT1-MMP at Invadopodia

(A–I′) MDA-MB-231 cells treated with mock (A–C′), VAMP7 (duplexB) (D–F′), and MT1-MMP siRNA (G–I′) were plated on fluorescently labeled gelatin (C, C′, F, F′, I, and I′) and stained with phalloidin (A, A′, D, D′, G, and G′) and cortactin antibodies (B, B′, E, E′, H, and H′). Enlargements of boxed regions are shown in (A′), (B′), (C′), (D′), (E′), (F′), (G′), (H′), and (I′) for the corresponding image. The scale bar in (A) (valid for [A], [B], [C], [D], [E], [F], [G], [H], and [I]) represents 10 μm; the scale bar in (A′) (valid for [A′], [B′], [C′], [D′], [E′], [F′], [G′], [H′], and [I′]) represents 2 μm.

(J) Quantification of gelatin degradation of MDA-MT1ch and MDA-MB-231 cells. Values are means ± standard errors of means (percentage ± SEM) of normalized degradation area.

(K) Results of transwell migration and invasion assay. MDA-MB-231 cells treated with mock and VAMP7 (duplexB) siRNA and mock-treated MDA-MT1ch cells as indicated were quantified after Transwell migration and invasion through Matrigel. Values are means ± SEM of normalized percentage.

(L) Results of invadopodia quantification. MDA-MB-231 cells of siRNA-treated populations as indicated were scored for the presence of invadopodia identified as bright actin spots regardless of degradation and further classified according to the number of invadopodia per cell. Values represent means ± SEM (percentage).

place (Figure 3E, asterisk). These nearly immobile vesicles might represent primed vesicles that are ready to release their content [29]. Additionally, we observed tubulogenesis from large GFP-VAMP7- and MT1-MMP-mCherry-positive vesicular structures in the vicinity of the ventral plasma membrane (Movie S3), suggesting that transport intermediates were pinched off from LE/lysosomal compartments for trafficking of the protease to invadopodia. The high degree of colocalization of VAMP7 and MT1-MMP at sites of degradation suggests an important functional role for VAMP7 in targeted delivery of the protease underlying the mechanism of MT1-MMP accumulation at invadopodia.

Depletion of VAMP7 Impairs MT1-MMP-Dependent Degradation and Invasion

We investigated a specific role of VAMP7 for MT1-MMP-dependent ECM proteolysis. First, we analyzed the significance of MT1-MMP itself for matrix degradation in human cancer cells. MDA-MB-231 cells were efficiently knocked down with siRNAs specific to MT1-MMP (Figure S2A), and depletion of MT1-MMP completely abolished the capacity of these cells as well as MDA-MT1ch cells to degrade the matrix (Figures 4G–4I′ and 4J, and Figures S2D–S2D″), confirming the paramount importance of MT1-MMP in cellular invasiveness [4, 8, 9]. To address the relevance of VAMP7 in MT1-MMP-dependent degradation, we analyzed matrix proteolysis of MDA-MB-231 and MDA-MT1ch cells depleted for VAMP7. VAMP7 knockdown with two independent siRNAs (Figure S2A) resulted in ~60%–70% reduction in the degradative capacity of MDA-MB-231 cells as compared to mock-treated cells (Figures 4A–4F′ and 4J and Figures S2B–S2C″). Consistently, even in the background of stably overexpressed MT1-MMP-mCherry, depletion of VAMP7 with two different siRNAs inhibited matrix degradation to similar extents (Figure 4J). VAMP7 depletion from MDA-MB-231 cells did neither affect total protein levels of MT1-MMP (Figure S2E) nor change the preferential association to LE/lysosomes (data not shown). This implies that VAMP7 is required for efficient matrix proteolysis exerted by endogenous as well as ectopically expressed MT1-MMP.

To investigate cancer cell invasion through a stiff extracellular matrix, we compared mock-treated MDA-MB-231 cells with VAMP7-depleted MDA-MB-231 cells in a Matrigel transwell assay as a model of basement-membrane invasion. VAMP7 depletion resulted in a 40% reduced capacity to pass the Matrigel lattice as compared with mock-treated cells (Figure 4K). Of note, under similar conditions, MT1-MMP depletion led to 60% inhibition of invasion through Matrigel [16]. Conversely, stable overexpression of MT1-MMP-mCherry (MDA-MT1ch cells) increased the invasion capacity to 140% as compared with mock-treated cells (Figure 4K), confirming previous results [6, 7, 9]. We then tested the effect of VAMP7 loss of function on 3D migration in collagen I matrix. Mock and VAMP7-depleted cells were embedded in collagen I and analyzed by time-lapse microscopy. As already reported [30], mock-treated MDA-MB-231 cells displayed mainly a mesenchymal mode of migration (64% mesenchymal versus 36% amoeboid). On the contrary, VAMP7 depletion led to an inversion of phenotype (42% mesenchymal versus 58% amoeboid, see Figures S3A and S3B and Movie S4) and affected neither speed nor directional persistence of migration (Figure S4).

Altogether, our results are in agreement with recent data showing that invasion through 3D collagen matrix may be only partially dependent on pericellular proteolysis and that cells can switch from mesenchymal to amoeboid movement upon MMP inhibition [30, 31]. MT1-MMP-mediated pericellular proteolytic activity is required for cancer cells to breach the basal membrane and for mesenchymal migration in fibrillar collagen matrix [6, 9, 31]. Our observations that VAMP7 is important for both 3D mesenchymal migration in collagen I and invasion through reconstituted basement membrane as well as gelatin degradation strongly argue that VAMP7 is a pivotal regulator of MT1-MMP-mediated matrix degradation and invasion.

Invadopodia Formation Is Coupled to Its Proteolytic Machinery

Analysis of the structural components required for invadopodia formation revealed several components such as N-WASP, Arp2/3 complex, and cortactin, which constitute the actin polymerization machinery. Signaling molecules such as c-Src orchestrate the formation of invadopodia (for review, see [32]). Interestingly, it has been proposed recently that MT1-MMP expression and activity are required for formation and maturation of invadopodia in SCC61 squamous cell carcinoma and MDA-MB-231 cell lines [3, 4]. Thus, we wondered whether impairment of MT1-MMP exocytosis by VAMP7 depletion affected formation of invadopodia. We analyzed invadopodia formation in MDA-MB-231 cells plated on fluorescently labeled matrix, stained for filamentous actin and cortactin [3, 4]. In mock-treated cells, we readily observed invadopodia in which F-actin and cortactin staining perfectly colocalized (Figures 4A–4B′). In some instances, the gelatin degradation was even broader (Figures 4C and 4C′), corresponding to previous sites of proteolytic degradation no longer associated with invadopodia as described [33]. Notably, the intensity and number of F-actin and cortactin doubly stained structures was decreased in VAMP7-depleted cells (Figures 4D–4E′), and these were associated with reduced proteolysis of the underlying matrix (Figures 4F and 4F′). In MT1-MMP-depleted cells, invadopodia were strongly reduced (Figures 4G–4H′), and matrix proteolysis was abolished (Figures 4I and 4I′; see also Figures S2B–S2D″). Quantification of invadopodia resulted in 19% of mock-treated cells displaying invadopodia, whereas this number was reduced to 8%–9% in VAMP7-depleted cells and less than 5% of MT1-MMP-siRNA-treated cells (Figure 4L). The number of invadopodia per cell was greatly reduced in VAMP7 cells, although not as strongly affected as in MT1-MMP-siRNA-treated cells (Figure 4L). Strikingly, VAMP7-depleted cells showed reduced amount of surface MT1-MMP clusters at the extracellular site of invadopodia, although total MT1-MMP levels were not

(M–P′) MDA-MB-231 cells treated with mock (M–N′) or VAMP7 siRNA (duplexB) (O–P′) were subjected to surface labeling with MT1-MMP antibodies. Enlargements of regions boxed in (M) and (O) are shown in (M′), (N′), (O′), and (P′) for the corresponding image. The scale bar in (M) (valid for [M], [N], [O], and [P]) represents 10 μm, and the scale bar in (M′) (valid for [M′], [N′], [O′], and [P′]) represents 2 μm.

(Q) Quantification of surface MT1-MMP accumulation. MDA-MB-231 cells of siRNA-treated populations as indicated were scored for the presence of surface MT1-MMP clusters at the ventral plasma membrane in contact with the matrix, regardless of degradation. Values represent mean percentage ± SEM. Differences between all siRNA-treated populations and respective mock populations from all quantifications were confirmed to be statistically significant (see Table S1). The number of experiments (N) and total number of cells (n) are indicated.

affected (see Figures 4M–4P′ and Figure S2E; 18% of mock-treated cells showed MT1-MMP accumulations at the ventral plasma membrane versus 5%–8% in VAMP7-siRNA-treated cells, Figure 4Q). Altogether, the data presented here strongly argue for VAMP7 being a critical SNARE during directed delivery of MT1-MMP to invadopodia. Furthermore, our findings that prevention of MT1-MMP delivery (VAMP7 siRNA) or expression (MT1-MMP siRNA) led to reduced invadopodia number agree with recent reports suggesting that MT1-MMP contributes to invadopodia formation and/or maturation [3, 4]; i.e., invadopodia formation in VAMP7-depleted cells is blocked or arrested in a premature state, at which accumulation of the protease is blocked.

The paramount importance of MT1-MMP for cancer cell invasion is well documented [7–9]. We addressed here the question of how the protease is localized to sites of matrix proteolysis and connect for the first time a v-SNARE to its cargo MT1-MMP. VAMP7 and MT1-MMP are colocalized at proteolytic sites; furthermore, depletion of VAMP7 phenocopied partially the effect of MT1-MMP depletion from cancer cells, leading to reduced degradative and invasive capacities. Strikingly, silencing of VAMP7 resulted in a reduced invadopodia number, which was accompanied by significantly lesser amounts of MT1-MMP accumulated at the ventral side of the cells facing the ECM. Finally, loss of VAMP7 resulted in a switch from mesenchymal to amoeboid mode of migration. Altogether, these data identify VAMP7 as a key cellular factor necessary for MT1-MMP-dependent matrix degradation, suggesting LE/lysosomal exocytosis to be an important process for matrix degradation by tumor cells. Beyond its relevance for signaling leading to known consequences for actin polymerization at invadopodia, our study pinpoints membrane trafficking as an essential component of the mechanisms of invadopodia formation and activity.

Supplemental Data

Experimental Procedures, four figures, one table, and four movies are available at http://www.current-biology.com/cgi/content/full/18/12/926/DC1/.

Acknowledgments

We are grateful to M.C. Rio (IGBMC, Illkirch, France) for sharing the monoclonal MT1-MMP antibody. We would like to thank P. Friedl and K. Wolf (University of Würzburg, Germany) for their help in setting up the migration assay in 3D Collagen. We are indebted to the Cell and Tissue Imaging facility (PICT-IBiSA) of CNRS/Institut Curie for help with image processing. This work was supported by grants from Institut Curie, CNRS, Agence Nationale de la Recherche (ANR), Ligue Nationale contre le Cancer "Equipe Labellisée," and Fondation BNP-Paribas (to P.C.). R.P. was supported by a grant of Association pour la Recherche contre le Cancer and Institut National du Cancer. K.R. acknowledges support by the Deutsche Forschungsgemeinschaft. A.S. was supported by Institut Curie and EMBO (ALTF 319-2006).

Received: February 21, 2008
Revised: May 22, 2008
Accepted: May 23, 2008
Published online: June 19, 2008

References

1. Linder, S. (2007). The matrix corroded: Podosomes and invadopodia in extracellular matrix degradation. Trends Cell Biol. *17*, 107–117.
2. Buccione, R., Orth, J.D., and McNiven, M.A. (2004). Foot and mouth: Podosomes, invadopodia and circular dorsal ruffles. Nat. Rev. Mol. Cell Biol. *5*, 647–657.
3. Clark, E.S., Whigham, A.S., Yarbrough, W.G., and Weaver, A.M. (2007). Cortactin is an essential regulator of matrix metalloproteinase secretion and extracellular matrix degradation in invadopodia. Cancer Res. *67*, 4227–4235.
4. Artym, V.V., Zhang, Y., Seillier-Moiseiwitsch, F., Yamada, K.M., and Mueller, S.C. (2006). Dynamic interactions of cortactin and membrane type 1 matrix metalloproteinase at invadopodia: Defining the stages of invadopodia formation and function. Cancer Res. *66*, 3034–3043.
5. Sato, T., del Carmen Ovejero, M., Hou, P., Heegaard, A.M., Kumegawa, M., Foged, N.T., and Delaisse, J.M. (1997). Identification of the membrane-type matrix metalloproteinase MT1-MMP in osteoclasts. J. Cell Sci. *110*, 589–596.
6. Hotary, K., Li, X.Y., Allen, E., Stevens, S.L., and Weiss, S.J. (2006). A cancer cell metalloprotease triad regulates the basement membrane transmigration program. Genes Dev. *20*, 2673–2686.
7. Hotary, K.B., Allen, E.D., Brooks, P.C., Datta, N.S., Long, M.W., and Weiss, S.J. (2003). Membrane type I matrix metalloproteinase usurps tumor growth control imposed by the three-dimensional extracellular matrix. Cell *114*, 33–45.
8. Ueda, J., Kajita, M., Suenaga, N., Fujii, K., and Seiki, M. (2003). Sequence-specific silencing of MT1-MMP expression suppresses tumor cell migration and invasion: Importance of MT1-MMP as a therapeutic target for invasive tumors. Oncogene *22*, 8716–8722.
9. Sabeh, F., Ota, I., Holmbeck, K., Birkedal-Hansen, H., Soloway, P., Balbin, M., Lopez-Otin, C., Shapiro, S., Inada, M., Krane, S., et al. (2004). Tumor cell traffic through the extracellular matrix is controlled by the membrane-anchored collagenase MT1-MMP. J. Cell Biol. *167*, 769–781.
10. Remacle, A., Murphy, G., and Roghi, C. (2003). Membrane type I-matrix metalloproteinase (MT1-MMP) is internalised by two different pathways and is recycled to the cell surface. J. Cell Sci. *116*, 3905–3916.
11. Jiang, A., Lehti, K., Wang, X., Weiss, S.J., Keski-Oja, J., and Pei, D. (2001). Regulation of membrane-type matrix metalloproteinase 1 activity by dynamin-mediated endocytosis. Proc. Natl. Acad. Sci. USA *98*, 13693–13698.
12. Uekita, T., Itoh, Y., Yana, I., Ohno, H., and Seiki, M. (2001). Cytoplasmic tail-dependent internalization of membrane-type 1 matrix metalloproteinase is important for its invasion-promoting activity. J. Cell Biol. *155*, 1345–1356.
13. Wu, X., Gan, B., Yoo, Y., and Guan, J.L. (2005). FAK-mediated src phosphorylation of endophilin A2 inhibits endocytosis of MT1-MMP and promotes ECM degradation. Dev. Cell *9*, 185–196.
14. Lafleur, M.A., Mercuri, F.A., Ruangpanit, N., Seiki, M., Sato, H., and Thompson, E.W. (2006). Type I collagen abrogates the clathrin-mediated internalization of membrane type 1 matrix metalloproteinase (MT1-MMP) via the MT1-MMP hemopexin domain. J. Biol. Chem. *281*, 6826–6840.
15. Bravo-Cordero, J.J., Marrero-Diaz, R., Megias, D., Genis, L., Garcia-Grande, A., Garcia, M.A., Arroyo, A.G., and Montoya, M.C. (2007). MT1-MMP proinvasive activity is regulated by a novel Rab8-dependent exocytic pathway. EMBO J. *26*, 1499–1510.
16. Sakurai-Yageta, M., Sibarita, J.B., Daviet, L., Camonis, J., D'Souza-Schorey, C., and Chavrier, P. (2008). The interaction of IQGAP1 with the exocyst complex is required for breast tumor cell invasion downstream of Cdc42 and RhoA. J. Cell Biol., in press.
17. Jahn, R., and Scheller, R.H. (2006). SNAREs–engines for membrane fusion. Nat. Rev. Mol. Cell Biol. *7*, 631–643.
18. Hong, W. (2005). SNAREs and traffic. Biochim. Biophys. Acta *1744*, 493–517.
19. Bonifacino, J.S., and Glick, B.S. (2004). The mechanisms of vesicle budding and fusion. Cell *116*, 153–166.
20. Galli, T., Zahraoui, A., Vaidyanathan, V.V., Raposo, G., Tian, J.M., Karin, M., Niemann, H., and Louvard, D. (1998). A novel tetanus neurotoxin-insensitive vesicle-associated membrane protein in SNARE complexes of the apical plasma membrane of epithelial cells. Mol. Biol. Cell *9*, 1437–1448.
21. Advani, R.J., Yang, B., Prekeris, R., Lee, K.C., Klumperman, J., and Scheller, R.H. (1999). VAMP-7 mediates vesicular transport from endosomes to lysosomes. J. Cell Biol. *146*, 765–776.
22. Alberts, P., Rudge, R., Irinopoulou, T., Danglot, L., Gauthier-Rouviere, C., and Galli, T. (2006). Cdc42 and actin control polarized expression of TI-VAMP vesicles to neuronal growth cones and their fusion with the plasma membrane. Mol. Biol. Cell *17*, 1194–1203.
23. Arantes, R.M., and Andrews, N.W. (2006). A role for synaptotagmin VII-regulated exocytosis of lysosomes in neurite outgrowth from primary sympathetic neurons. J. Neurosci. *26*, 4630–4637.

24. Randhawa, V.K., Thong, F.S., Lim, D.Y., Li, D., Garg, R.R., Rudge, R., Galli, T., Rudich, A., and Klip, A. (2004). Insulin and hypertonicity recruit GLUT4 to the plasma membrane of muscle cells by using N-ethylmaleimide-sensitive factor-dependent SNARE mechanisms but different v-SNAREs: Role of TI-VAMP. Mol. Biol. Cell *15*, 5565–5573.
25. Pocard, T., Le Bivic, A., Galli, T., and Zurzolo, C. (2007). Distinct v-SNAREs regulate direct and indirect apical delivery in polarized epithelial cells. J. Cell Sci. *120*, 3309–3320.
26. Braun, V., Fraisier, V., Raposo, G., Hurbain, I., Sibarita, J.B., Chavrier, P., Galli, T., and Niedergang, F. (2004). TI-VAMP/VAMP7 is required for optimal phagocytosis of opsonised particles in macrophages. EMBO J. *23*, 4166–4176.
27. Boucrot, E., and Kirchhausen, T. (2007). Endosomal recycling controls plasma membrane area during mitosis. Proc. Natl. Acad. Sci. USA *104*, 7939–7944.
28. Proux-Gillardeaux, V., Rudge, R., and Galli, T. (2005). The tetanus neurotoxin-sensitive and insensitive routes to and from the plasma membrane: Fast and slow pathways? Traffic *6*, 366–373.
29. Nofal, S., Becherer, U., Hof, D., Matti, U., and Rettig, J. (2007). Primed vesicles can be distinguished from docked vesicles by analyzing their mobility. J. Neurosci. *27*, 1386–1395.
30. Wolf, K., Mazo, I., Leung, H., Engelke, K., von Andrian, U.H., Deryugina, E.I., Strongin, A.Y., Brocker, E.B., and Friedl, P. (2003). Compensation mechanism in tumor cell migration: Mesenchymal-amoeboid transition after blocking of pericellular proteolysis. J. Cell Biol. *160*, 267–277.
31. Wolf, K., Wu, Y.I., Liu, Y., Geiger, J., Tam, E., Overall, C., Stack, M.S., and Friedl, P. (2007). Multi-step pericellular proteolysis controls the transition from individual to collective cancer cell invasion. Nat. Cell Biol. *9*, 893–904.
32. Weaver, A.M. (2006). Invadopodia: Specialized cell structures for cancer invasion. Clin. Exp. Metastasis *23*, 97–105.
33. Bowden, E.T., Onikoyi, E., Slack, R., Myoui, A., Yoneda, T., Yamada, K.M., and Mueller, S.C. (2006). Co-localization of cortactin and phosphotyrosine identifies active invadopodia in human breast cancer cells. Exp. Cell Res. *312*, 1240–1253.